Author Manuscript

Author Manuscript

Author Manuscript

Author Manuscript

HHS Public Access

Author manuscript

Biochemistry. Author manuscript; available in PMC 2015 May 25.

Published in final edited form as:

Biochemistry. 2006 March 21; 45(11): 3473–3480. doi:10.1021/bi052638z.

Hydration of the folding transition-state ensemble of a protein

Ludovic Brun[1], **Daniel G. Isom**[2], **Priya Velu**[2], **Bertrand García-Moreno**[2], and **Catherine Royer**[1]

[1] INSERM U554, Centre de Biochimie Structurale, Montpellier, France

[2] Department of Biophysics, Johns Hopkins University, Baltimore MD 21218, USA

Abstract

A complete description of the mechanisms of protein folding requires knowledge of the structural and physical character of the folding transition state ensembles (TSE). A key question remains, concerning the role of hydration of the hydrophobic core in determining folding mechanisms. To address this we probed the state of hydration of the TSE of staphylococcal nuclease (SNase) by examining the fluorescence-detected pressure-jump relaxation behavior of six SNase variants in which a residue in the hydrophobic core, Val-66, was replaced with polar or ionizable residues (Lys, Arg, His, Asp, Glu, Asn). Owing to a large positive activation volume for folding, the major effect of pressure on the wild type protein is to decrease the folding rate. By the time wild type SNase reaches the folding transition state, most water has already been expelled from its hydrophobic core. In contrast, the major effect of pressure on the variant proteins is an increase of the unfolding rate due to a large negative activation volume for unfolding. This results from a significant increase in the hydration of the TSE when an internal ionizable group is present. These data confirm that the role of water in the folding reaction can differ from protein to protein, and that even a single substitution in a critical position can modulate significantly the properties of the TSE.

The exponential nature of protein folding kinetics suggests the existence of rate-limiting energy barriers between the folded and the unfolded states. The lack of detailed understanding of this barrier and of the attendant rate-limiting ensemble of states still limits our ability to describe mechanisms of folding in detail. Although use of φ-value analysis (1–4) to describe the character of the folding transition state ensembles (TSE) remains controversial (5;6), a self-consistent view is emerging (7–12). Considerable differences in the TSE of different proteins have been observed (13;14), but in general, native-like structures are thought to dominate the TSE, possibly even with many side chains already fully dehydrated but with few of them satisfying their native contacts (5;6;15).

Computational analyses of φ values have influenced significantly the prevailing views on the structural character of the TSE (16–28), which is thought to be determined primarily by the topology of the protein, not by detailed energetic factors (17;24;29;30). Some computational studies suggest that TSEs consist mostly of expanded and distorted native

---

Correspondence to: Catherine Royer.

Author Manuscript Author Manuscript Author Manuscript Author Manuscript

structure. In MD-based studies, subsets of nucleating interactions are assigned key roles (19;21;22;27), but this is not fully consistent with experimental data (5;6;31).

Despite this progress in characterizing the TSE, the central question of the role of hydration in determining folding rates and mechanisms remains unanswered. Computational studies suggest that the conformations populated in the TSE consist mostly of native structure with a highly solvated hydrophobic core. The final step in the folding reaction is thought to involve packing of the hydrophobic core and concomitant, cooperative squeezing out of water from the core (16;20;25;32). Water in the core of the TSE could prevent nonnative contacts from being formed (28). Experimentally it has been shown that replacement of a hydrophobic core sidechain with an isosteric polar one can alter the hydration of the TSE when residues crucial to the folding mechanism are targeted (32). These experimental findings can be modeled using a desolvation potential (16). They support the view of the TSE as a highly hydrated state.

The emerging view of TSEs as a highly hydrated, native-like state is not consistent with previous results from pressure-jump relaxation studies of wild type (WT) staphylococcal nuclease (SNase) (33). These studies revealed that the rate-limiting step in folding was accompanied by significant dehydration, and that the TSE for this protein was relatively dry. Indeed, pressure perturbation offers a unique experimental means for probing the role of hydration changes in protein conformational changes (34) because pressure effects arise from differences in the specific volumes of the various (folded, intermediates, unfolded, transition) states of the protein. These differences in specific volume are linked directly to the degree and type (polar or non-polar) of hydration, and to the existence or loss of cavity volume (35;36), which also involve hydration or dehydration, respectively. Most proteins studied to date exhibit a larger specific volume in the folded state than in the unfolded state, hence the application of pressure leads to their unfolding. Our earlier p-jump relaxation studies demonstrated that the effect of pressure on the stability of WT SNase arises primarily from a pressure-induced decrease in the folding rate constant due to a positive activation volume for this reaction, suggesting significant dehydration of the transition state ensemble (33). Similar p-jump relaxation studies on the folding of six other proteins indicated that significant (although less) dehydration accompanied the rate-limiting step in folding of these proteins as well (37–42).

To probe the state of hydration of the TSE of SNase in depth, we performed pressure unfolding experiments with variants in which a deeply buried hydrophobic residue, Val-66, was replaced with Arg, Lys, His, Asp, Glu, or Asn. Charged and polar groups are well hydrated in water, therefore removal of these groups from water for placement into the core of the protein is energetically unfavorable. The introduction of ionizable and polar groups in the protein interior were expected to perturb the TSE of the protein, and to allow clarification of the role of water in the final stages of folding with unprecedented level of detail.

Author Manuscript Author Manuscript Author Manuscript Author Manuscript

METHODS

Replacement of core hydrophobic positions with polar or ionizable residues is energetically disfavored (43–50). For this reason, the variants with the internal position Val-66 substituted with Arg, Lys, His, Asp, Glu, or Asn were engineered using a hyperstable form of SNase known as Δ+PHS after the set of substitutions (P117G, H124L, S128A, G50F, V51N) and deletions (Δ44–49). WT SNase and all of the Δ+PHS proteins were produced and purified as described previously (51). The pressure-jump experiments were carried out in either Tris or bis-Tris buffer (Aldrich) 50 mM at the pH indicated in Table 1 to avoid pressure-induced changes in the pH (52). GuHCl (Aldrich) was dissolved into the appropriate buffer, the pH adjusted and used at the concentration indicated in Table 1. Protein concentration was near 70 μM.

High pressure experiments were carried out using a stainless steel high pressure cell designed in our laboratory and fitted with sapphire windows. The high pressure generating equipment has been previously described (53). High purity (18 MOhm) water was used as the pressure generating liquid. Fluorescence measurements were made using the detection from an ISS KOALA instrument (ISS Champaign IL) and ISS excitation source and monochromator coupled to the high pressure cell via an optical fiber. The excitation and emission monochromator slits were at 8 nm and the excitation wavelength was 295 nm, while the emission was set at 335 nm. Emission spectra (310–450 nm) were also acquired once the sample had equilibrated. The acquisition time base was 1 second. Pressure jumps were performed by pumping the pressure with the valve to the high pressure cell closed, followed by rapid opening of the valve. Solution conditions were adjusted with pH or guanidine hydrochloride to decrease the stability of the proteins so that pressures below 4 kbar (400 MPa) were sufficient to unfold the variants tested. We have shown previously that changes in pH or in the concentration of GuHCl change the stability of SNase without affecting the volume change measured by pressure unfolding (53;54).

Equilibrium unfolding profiles were analyzed for the volume change (ΔV_f) and free energy of folding (ΔG_f) using the analysis program Bioeqs and an analytical rather than numerical model of 2-state folding.

$$\frac{d\Delta G_f}{\mathrm{dp}} = -\Delta V_f \quad (1)$$

$$\Delta G_f = -\mathrm{RT}\ln K_f \quad (2)$$

$$K_f = \frac{[F]}{[U]} = \frac{(I_p - I_i)}{(I_i - I_p)} \quad (3)$$

Uncertainties on the recovered free energy and volume change values were determined by rigorous confidence limit testing, and take into account correlations between the fitted parameter.

Author Manuscript Author Manuscript Author Manuscript Author Manuscript

The pressure-jump relaxation profiles at each pressure were analyzed according to classical transition state theory for a single exponential decay:

$$I_{(t)}=I_o e^{-\frac{t}{\tau(p)}}+C \quad (4)$$

For a simple two state reaction, the relaxation time τ at each pressure is the inverse sum of the folding and unfolding rate constants $k_{f(p)}$ *and* $k_{u(p)}$ at that pressure.

$$\ln\tau_{(p)}=1/(k_{f(p)}+k_{u(p)}) \quad (5)$$

These rate constants are exponentially dependent upon pressure and the activation volumes for the reactions.

$$k_{f(p)}=k_{fo}e^{-p\Delta V_f^{\neq}/RT} \text{ and } k_{u(p)}=k_{uo}e^{-p\Delta V_u^{\neq}/RT} \quad (6)$$

Thus the plots of *ln* τ vs *p* are fit using non-linear least squares analysis for the values of the activation volumes ($\Delta V^{\neq}_f$ and $\Delta V^{\neq}_u$) and rate constants (k_{fo} and k_{uo}) for folding and unfolding at atmospheric pressure. We have constrained the analysis to only two parameters, either those for folding (WT) or unfolding (variants), using the equilibrium volume change and free energy for folding according to

$$\Delta G_f^o=-RT\ln K_f=-RT\ln\frac{k_f}{k_u} \quad (7)$$

such that

$$k_f=k_u K_f \text{ or } k_u=\frac{K_f}{k_f} \quad (8)$$

and

$$\Delta V_f^o=\Delta V_f^{\neq}-\Delta V_u^{\neq} \quad (9)$$

such that

$$\Delta V_f^{\neq}=\Delta V_f^o-\Delta V_u^{\neq} \quad \text{or} \quad \Delta V_u^{\neq}=\Delta V_f^{\neq}-\Delta V_f^o. \quad (10)$$

Uncertainties reported are calculated from the diagonal of the correlation matrix and correspond to 95% confidence limits.

Author Manuscript Author Manuscript Author Manuscript Author Manuscript

RESULTS AND DISCUSSION

Proteins with internal polar or ionizable residues

Fluorescence-detected pressure-jump relaxation experiments were performed with V66K, V66R, V66H, V66D, V66E, and V66H variants of the Δ+PHS hyperstable nuclease. Crystal structures of all but the His-66 variant have been determined previously under room temperature and cryogenic conditions (Figure 1) (45;47;48;50;55). With the exception of the V66R variant, in which the β-barrel releases a strand to expose Arg-66 to water (Karp, Gittis, & García-Moreno, in preparation), under conditions near neutral pH, where the internal ionizable groups are neutral, the residues at position-66 are indeed buried in the core of the protein in a hydrophobic pocket. Under these conditions there are also no detectable differences between the native states of the variant proteins and of the background protein. One or two internal water molecules have been observed hydrating the internal polar moieties in cryogenic structures with internal Asp, Glu, Asn, Gln, Tyr, and Trp at position 66. Molecular dynamics simulations also suggest that 2 or 3 water molecules can penetrate into the hydrophobic core of WT SNase at room temperature and pressure, even in the absence of internal polar or ionizable groups (56). Internal water molecules have never been observed crystallographically in the WT protein.

The pKa values of the internal ionizable groups have been measured previously: 5.7 for Lys-66 (46–48), 8.9 for Asp-66 (48), 9.2 for Glu-66 (45), < 4 for His-66, >10 for Arg-66 (Karp, Gittis, Garcia-Moreno, in preparation). These pKa values are shifted substantially relative to the pKa values of ionizable groups in water. This effect is driven largely by the dehydration of the ionizable groups when they are in internal positions in the protein (46).

Equilibrium Unfolding by Pressure

The fluorescence-detected pressure-induced unfolding profiles of wild type and variant Snase (Figure 2) were fit to a 2-state unfolding model. The values for the volume change and free energy for folding at atmospheric pressure (ΔV^o_f and ΔG^o_f) recovered from this analysis are listed in Table 1. The ΔV^o_f for wild-type SNase is within error of our previously reported measurement of 70 ±10 ml/mol (at 21 rather than 23 °C) (33;57). The volume change for folding the Δ+PHS was 41 ml/mol, significantly smaller than that of the wild-type. The substitutions and deletions used to create the Δ+PHS hyperstable form of SNase are at external sites and produce only local changes in the structure (43;44). We have also shown previously that the P117G+H124L double substitution has no effect on the volume change of unfolding (54). The other mutations and deletions in Δ+PHS are unlikely to result in significant structural changes since they are all exposed. Hence, the difference in overall volume change between the Δ+PHS and WT SNase must arise from stabilization of residual structure in the unfolded state in the Δ+PHS variant. Clearly introduction of ionizable residues in the hydrophobic core disrupts this residual structure in the unfolded state, rendering the overall volume change upon unfolding comparable to that of the WT Snase.

With the exception of Arg-66, the other internal ionizable groups were largely neutral under the conditions tested (45;46;48). We expected a contribution to the pressure effects from the electrostriction related to the ionization of these internal ionizable residues upon unfolding.

Author Manuscript Author Manuscript Author Manuscript Author Manuscript

This should have led to an increase the magnitude of the ΔV^o_f above that of the background Δ+PHS protein. While the variants with V66K, V66E, and V66D all exhibited ΔV^o_f values greater than for the Δ+PHS background protein, consistent with electrostriction, those with V66R, V66H, and V66N unfold with ΔV^o_f values that are as large or even larger than for the proteins in which electrostriction was anticipated, and yet in these variants electrostriction cannot be a factor because these groups are either neutral (His, Asn) or charged (Arg) in both folded and unfolded states at the pH where the experiments were performed. Although we have shown previously that an increase in the size of the small internal cavity around position 66 will result in larger ΔV^o_f values (35), this also cannot be the reason behind the larger ΔV^o_f values measured for the variants with internal polar and ionizable side chains because these side chains would actually decrease the volume of the small internal cavity. Instead, the large ΔV^o_f must reflect the destabilization of residual structure in the unfolded state. We note that the free energy values cannot be compared among variants since the conditions of the experiments were chosen in order to tune the pressure-induced unfolding into the appropriate range for our apparatus. However, the free energy measured by pressure and chemical denaturation for all variants are in agreement (data for chemical denaturation not shown), corroborating the validity of the thermodynamic parameters obtained by pressure unfolding.

Pressure-jump relaxation kinetics

Pressure-jump relaxation profiles at multiple pressures were obtained for all the variants. The Δ+PHS protein was not studied because the relaxation was faster than the 2 s dead time of our instrument. This very fast relaxation time is consistent with a large increase in the folding rate for this hyperstable variant. All of the other variants exhibited single exponential relaxation curves, indicative of simple 2-state kinetic behavior, as has been shown previously for WT SNase at high pressure under a variety of conditions (33;57). This loss of kinetic complexity at high pressure appears to arise from the pressure inhibition of proline isomerization (54;58).

For WT SNase (Figure 3a) the relaxation times increase significantly with increasing pressure, as previously reported (33;57). Strikingly, the V66K, V66R, V66D and V66E variants of Δ+PHS exhibited the opposite behavior (shown in Figure 3b for the Δ+PHS/V66K variant). As pressure was increased, the relaxation times became significantly shorter. The relaxation profiles at each pressure for each variant were analyzed for a single exponential relaxation time. Plots of the natural logarithm of these relaxation times ($ln\ \tau$ *vs.* pressure) are shown in Figure 4 for WT SNase and for the V66N, V66K, V66R, V66D, and V66E variants of Δ+PHS. The $ln\ \tau$ *vs.* pressure plots for all of the variants were analyzed according to equations (5) and (6) for the activation volumes and rate constants for either folding or unfolding.

The analysis for the WT protein yielded, as previously reported, a large activation volume for folding and a very small negative activation volume for unfolding (Table 1). In contrast, for the V66K, V66R, V66D, and V66E variants, the activation volume for folding was much smaller than for the wild type protein, while that for unfolding was very large and negative (Figure 4, Table 2).

Author Manuscript Author Manuscript Author Manuscript Author Manuscript

The differences in folding mechanisms of wild type and variant proteins are described schematically by the volume diagrams in Figure 5. The activation volumes for folding and unfolding combine to yield the overall equilibrium volume changes. The equilibrium unfolding volume changes are somewhat different among the variants tested here. Because the structures of the native state are comparable for the proteins studied, the differences in equilibrium volume change must be linked to differences in the degree of hydration of the unfolded state. In the case of the wild type protein, the volume of the TSE lies near that of the folded state. This is consistent with our prior interpretation that the TSE of WT SNase is highly dehydrated (33;57). In contrast, the V66K variant exhibits a TSE whose volume is much closer to that of the unfolded state, and thus much more hydrated that the WT TSE. For the V66N andV66E the equilibrium unfolding volume change is larger than for the other variants. Since there are no significant structural differences among the native states of these proteins, this is also more likely to reflect increased hydration of the unfolded state. Also since the folded states of the Δ+PHS background variant and the WT Snase are structurally equivalent, and the Δ+PHS mutant is significantly more stable than the WT, it is highly unlikely that these background stabilizing mutations are responsible for the more open, hydrated transition state observed in the variants of Δ+PHS bearing ionizable residues in their hydrophobic core.

The analysis of the pressure-jump relaxation data presented above is grounded on classical transition state theory. The kinetic and energetic basis of pressure-induced protein unfolding has also been analyzed previously (59) with energy landscape theory of protein folding (60), using a square well potential that includes a desolvation barrier (61;62). In this theoretical treatment of a model β-barrel protein, increasing pressure was found to actually lower the transition barrier. Nevertheless, the overall result of pressure was to decrease the folding rate because of a large effect of pressure on the reconfigurational diffusion coefficient, D_Q. This pressure-induced decrease in D_Q suggests that in these simulations, the increase in the rate of folding by increasing pressure was surpassed by the increase in the roughness of the landscape with increasing pressure. We have evidence from iso-energetic pressure studies of WT Snase at varying concentrations of stabilizers and denaturants ((57); Frye, Niemeyer, Royer, Garcia and Onuchic, unpublished data) that pressure may indeed diminish the pre-exponential factor by a factor of 1.7/kbar. However, the overall decrease in the folding rate, over 1 kbar, represents a factor of 7 (Figure 4), demonstrating that pressure indeed increases the free energy at the folding barrier for this protein. The contribution of the pre-exponential factor is, at most, about 25% of the total effect of pressure in this system. In the case of the variants with internal ionizable residues, pressure leads to an increase of the relaxation rate, rather than slowing it down. A general effect of pressure on the roughness of the folding landscape cannot be invoked to explain our observations. Indeed, pressure may also decrease the D_Q in the case of the variants studied here, but this effect, if it exists, is compensated by a pressure-induced increase in the unfolding rate constant linked to a large, negative activation volume for unfolding.

CONCLUSIONS

The pressure-jump relaxation experiments have revealed a striking and unique difference in the folding mechanisms of wild type SN and of variants with internal polar or ionizable

Author Manuscript Author Manuscript Author Manuscript Author Manuscript

groups. Consider as a representative example the case of the V66K variant. The structure of the V66K variant of SNase is essentially identical to structure of the wild type protein (47;50). Under the conditions in which pressure unfolding was performed, the stability of the V66K protein and of its parent protein are quite similar, and the rate constants for folding and unfolding differ only by factors of 10 and 3 respectively. Even the equilibrium pressure unfolding profiles of the two proteins are almost indistinguishable. Yet the pressure dependence of their folding kinetics suggests that these two proteins fold via very different mechanisms.

The differences in the state of hydration of the TSE in the variants and in the wild type protein can be rationalized in terms of the high unfavorable free energy that would be required to neutralize and dehydrate a charged side chain if it were to be buried in a native-like TSE. Internal polar and ionizable groups would promote a hydrated TSE in which the polar and ionizable group destined to occupy internal positions in the native state can remain charged and fully solvated. The pressure unfolding data of the variants with internal polar or ionizable groups is very significant because it reinforces the view that the TSE of wild type SNase is highly dehydrated.

In many computational studies, based primarily on Go models and desolvation potentials, the native structure is achieved before water is expelled from the hydrophobic core (16;20;25;28;32). This would appear to be inconsistent with our observations of a highly dehydrated TSE for WT SNase. It is important to note that not all proteins behave the same way. Wild type SNase (33) and CspB (38), for example, appear to have highly dehydrated TSEs. The other five proteins that have been examined by pressure unfolding (*trp* repressor (37), $P13^{MTCP1}$ (39), CI2 (40), tendamistat (41), and P23 (42)) exhibit specific volumes for their TSEs that lie one half to three/fourths of the way between those of the unfolded and folded states. This is consistent with the TSEs of these proteins having lost water relative to the unfolded state, but nonetheless remaining significantly hydrated. Indeed in replica exchange MD simulations of the folding of protein A (61), about 25% of the hydrating waters remain at the TSE, and are expelled in the final step in folding. This amount of water remaining in the core at the TSE is actually in quite good agreement with the results of the pressure relaxation studies, in which 50–75% of the water is expelled at the TSE, leaving about 25%–50% behind. Wild type SNase appears to be somewhat of an exception (perhaps due to the important size of its hydrophobic core compared to most of the other proteins studied by p-jump techniques) - its TSE appears to be much closer to that of the native state than is observed in other proteins. We note as well that the activation and equilibrium volume changes calculated from the pressure effects on folding are indicative of the overall (thermodynamic) degree of hydration, and are not a quantitative measure of the number of water molecules, such that a direct comparison between the simulations and the experiments is not yet possible, particularly since they were not performed on the same protein systems.

The present results demonstrate that substitution of a single amino acid can drastically alter the state of hydration of the TSE. The role of hydration in determining folding mechanism is likely to be highly sequence dependent, and influenced by the presence of uncompensated polarity in the protein interior. These data also illustrate the high plasticity of the TSE, which apparently adapts structurally to an energetically costly change in sequence. In the

Author Manuscript Author Manuscript Author Manuscript Author Manuscript

case of wild type SNase, the folding TSE is already quite dehydrated, thus the last step in folding does not involve major dehydration of the hydrophobic core. Instead, it might involve the establishment of the native contacts necessary to stabilize side chains in their native-like conformations in an already dehydrated core (5;6;15;31).

Acknowledgments

This work was supported by NIH (R01-GM61597) to BGME and support from INSERM and the COST Program to CAR.

Abbreviations

Snase	Staphylococcal nuclease
TSE	transition state ensemble

References

1. Grantcharova VP, Riddle DS, Santiago JV, Baker D. Important role of hydrogen bonds in the structurally polarized transition state for folding of the src SH3 domain. Nat Struct Biol. 1998; 5:714–720. [PubMed: 9699636]
2. Grantcharova VP, Riddle DS, Baker D. Long-range order in the src SH3 folding transition state. Proc Natl Acad Sci U SA. 2000; 97:7084–7089.
3. Otzen DE, Itzhaki LS, elMasry NF, Jackson SE, Fersht AR. Structure of the transition state for the folding/unfolding of the barley chymotrypsin inhibitor 2 and its implications for mechanisms of protein folding. Proc Natl Acad Sci U SA. 1994; 91:10422–10425.
4. Serrano L, Matouschek A, Fersht AR. The folding of an enzyme. III. Structure of the transition state for unfolding of barnase analysed by a protein engineering procedure. J Mol Biol. 1992; 224:805–818. [PubMed: 1569558]
5. Raleigh DP, Plaxco KW. The protein folding transition state: what are Phi-values really telling us? Protein Pept Lett. 2005; 12:117–122. [PubMed: 15723637]
6. Sanchez IE, Kiefhaber T. Origin of unusual phi-values in protein folding: evidence against specific nucleation sites. J Mol Biol. 2003; 334:1077–1085. [PubMed: 14643667]
7. Grantcharova VP, Baker D. Circularization changes the folding transition state of the src SH3 domain. J Mol Biol. 2001; 306:555–563. [PubMed: 11178913]
8. Lindberg M, Tangrot J, Oliveberg M. Complete change of the protein folding transition state upon circular permutation. Nat Struct Biol. 2002; 9:818–822. [PubMed: 12368899]
9. Otzen DE, Kristensen O, Proctor M, Oliveberg M. Structural changes in the transition state of protein folding: alternative interpretations of curved chevron plots. Biochemistry. 1999; 38:6499–6511. [PubMed: 10350468]
10. Otzen DE, Oliveberg M. Correspondence between anomalous m- and DeltaCp-values in protein folding. Protein Sci. 2004; 13:3253–3263. [PubMed: 15557266]
11. Viguera AR, Serrano L, Wilmanns M. Different folding transition states may result in the same native structure. Nat Struct Biol. 1996; 3:874–880. [PubMed: 8836105]
12. Gruebele M. Protein folding: the free energy surface. Curr Opin Struct Biol. 2002; 12:161–168. [PubMed: 11959492]
13. Itzhaki LS, Otzen DE, Fersht AR. The structure of the transition state for folding of chymotrypsin inhibitor 2 analysed by protein engineering methods: evidence for a nucleation-condensation mechanism for protein folding. J Mol Biol. 1995; 254:260–288. [PubMed: 7490748]
14. Shen T, Hofmann CP, Oliveberg M, Wolynes PG. Scanning malleable transition state ensembles: comparing theory and experiment for folding protein U1A. Biochemistry. 2005; 44:6433–6439. [PubMed: 15850377]

Author Manuscript Author Manuscript Author Manuscript Author Manuscript

15. Frieden C. The kinetics of side chain stabilization during protein folding. Biochemistry. 2003; 42:12439–12446. [PubMed: 14580188]
16. Cheung MS, Garcia AE, Onuchic JN. Protein folding mediated by solvation: water expulsion and formation of the hydrophobic core occur after the structural collapse. Proc Natl Acad Sci U SA. 2002; 99:685–690.
17. Clementi C, Nymeyer H, Onuchic JN. Topological and energetic factors: what determines the structural details of the transition state ensemble and “en-route” intermediates for protein folding? An investigation for small globular proteins. J Mol Biol. 2000; 298:937–953. [PubMed: 10801360]
18. Ding F, Dokholyan NV, Buldyrev SV, Stanley HE, Shakhnovich EI. Direct molecular dynamics observation of protein folding transition state ensemble. Biophys J. 2002; 83:3525–3532. [PubMed: 12496119]
19. Gsponer J, Caflisch A. Molecular dynamics simulations of protein folding from the transition state. Proc Natl Acad Sci U S A. 2002; 99:6719–6724. [PubMed: 11983864]
20. Guo W, Lampoudi S, Shea JE. Posttransition state desolvation of the hydrophobic core of the src-SH3 protein domain. Biophys J. 2003; 85:61–69. [PubMed: 12829464]
21. Lindorff-Larsen K, Vendruscolo M, Paci E, Dobson CM. Transition states for protein folding have native topologies despite high structural variability. Nat Struct Mol Biol. 2004; 11:443–449. [PubMed: 15098020]
22. Lindorff-Larsen K, Rogen P, Paci E, Vendruscolo M, Dobson CM. Protein folding and the organization of the protein topology universe. Trends Biochem Sci. 2005; 30:13–19. [PubMed: 15653321]
23. Onuchic JN, Socci ND, Luthey-Schulten Z, Wolynes PG. Protein folding funnels: the nature of the transition state ensemble. Fold Des. 1996; 1:441–450. [PubMed: 9080190]
24. Shea JE, Onuchic JN, Brooks CL III. Exploring the origins of topological frustration: design of a minimally frustrated model of fragment B of protein A. Proc Natl Acad Sci U S A. 1999; 96:12512–12517. [PubMed: 10535953]
25. Sheinerman FB, Brooks CL III. Calculations on folding of segment B1 of streptococcal protein G. J Mol Biol. 1998; 278:439–456. [PubMed: 9571063]
26. Shoemaker BA, Wang J, Wolynes PG. Exploring structures in protein folding funnels with free energy functionals: the transition state ensemble. J Mol Biol. 1999; 287:675–694. [PubMed: 10092467]
27. Vendruscolo M, Paci E, Dobson CM, Karplus M. Three key residues form a critical contact network in a protein folding transition state. Nature. 2001; 409:641–645. [PubMed: 11214326]
28. Wu X, Brooks BR. Beta-hairpin folding mechanism of a nine-residue peptide revealed from molecular dynamics simulations in explicit water. Biophys J. 2004; 86:1946–1958. [PubMed: 15041639]
29. Scalley-Kim M, Baker D. Characterization of the folding energy landscapes of computer generated proteins suggests high folding free energy barriers and cooperativity may be consequences of natural selection. J Mol Biol. 2004; 338:573–583. [PubMed: 15081814]
30. Yi Q, Rajagopal P, Klevit RE, Baker D. Structural and kinetic characterization of the simplified SH3 domain FP1. Protein Sci. 2003; 12:776–783. [PubMed: 12649436]
31. Sanchez IE, Kiefhaber T. Evidence for sequential barriers and obligatory intermediates in apparent two-state protein folding. J Mol Biol. 2003; 325:367–376. [PubMed: 12488101]
32. Fernandez-Escamilla AM, Cheung MS, Vega MC, Wilmanns M, Onuchic JN, Serrano L. Solvation in protein folding analysis: combination of theoretical and experimental approaches. Proc Natl Acad Sci U S A. 2004; 101:2834–2839. [PubMed: 14978284]
33. Vidugiris GJ, Markley JL, Royer CA. Evidence for a molten globule-like transition state in protein folding from determination of activation volumes. Biochemistry. 1995; 34:4909–4912. [PubMed: 7711012]
34. Royer CA. Revisiting volume changes in pressure-induced protein unfolding. Biochim Biophys Acta. 2002; 1595:201–209. [PubMed: 11983396]

Author Manuscript Author Manuscript Author Manuscript Author Manuscript

35. Frye KJ, Perman CS, Royer CA. Testing the correlation between delta A and delta V of protein unfolding using m value mutants of staphylococcal nuclease. Biochemistry. 1996; 35:10234–10239. [PubMed: 8756489]
36. Frye KJ, Royer CA. Probing the contribution of internal cavities to the volume change of protein unfolding under pressure. Protein Sci. 1998; 7:2217–2222. [PubMed: 9792110]
37. Desai G, Panick G, Zein M, Winter R, Royer CA. Pressure-jump studies of the folding/unfolding of trp repressor. J Mol Biol. 1999; 288:461–475. [PubMed: 10329154]
38. Jacob MH, Saudan C, Holtermann G, Martin A, Perl D, Merbach AE, Schmid FX. Water contributes actively to the rapid crossing of a protein unfolding barrier. J Mol Biol. 2002; 318:837–845. [PubMed: 12054827]
39. Kitahara R, Royer C, Yamada H, Boyer M, Saldana JL, Akasaka K, Roumestand C. Equilibrium and pressure-jump relaxation studies of the conformational transitions of P13MTCP1. J Mol Biol. 2002; 320:609–628. [PubMed: 12096913]
40. Mohana-Borges R, Silva JL, Ruiz-Sanz J, de Prat-Gay G. Folding of a pressure-denatured model protein. Proc Natl Acad Sci U S A. 1999; 96:7888–7893. [PubMed: 10393917]
41. Pappenberger G, Saudan C, Becker M, Merbach AE, Kiefhaber T. Denaturant-induced movement of the transition state of protein folding revealed by high-pressure stopped-flow measurements. Proc Natl Acad Sci U S A. 2000; 97:17–22. [PubMed: 10618363]
42. Tan CY, Xu CH, Wong J, Shen JR, Sakuma S, Yamamoto Y, Lange R, Balny C, Ruan KC. Pressure Equilibrium and Jump Study on Unfolding of 23-kDa Protein from Spinach Photosystem II. Biophys J. 2005; 88:1264–1275. [PubMed: 15531632]
43. Baldisseri DM, Torchia DA, Poole LB, Gerlt JA. Deletion of the omega-loop in the active site of staphylococcal nuclease. 2 Effects on protein structure and dynamics. Biochemistry. 1991; 30:3628–3633. [PubMed: 2015220]
44. Chen J, Lu Z, Sakon J, Stites WE. Increasing the thermostability of staphylococcal nuclease: implications for the origin of protein thermostability. J Mol Biol. 2000; 303:125–130. [PubMed: 11023780]
45. Dwyer JJ, Gittis AG, Karp DA, Lattman EE, Spencer DS, Stites WE, Garcia-Moreno EB. High apparent dielectric constants in the interior of a protein reflect water penetration. Biophys J. 2000; 79:1610–1620. [PubMed: 10969021]
46. Fitch CA, Karp DA, Lee KK, Stites WE, Lattman EE, Garcia-Moreno EB. Experimental pK(a) values of buried residues: analysis with continuum methods and role of water penetration. Biophys J. 2002; 82:3289–3304. [PubMed: 12023252]
47. Garcia-Moreno B, Dwyer JJ, Gittis AG, Lattman EE, Spencer DS, Stites WE. Experimental measurement of the effective dielectric in the hydrophobic core of a protein. Biophys Chem. 1997; 64:211–224. [PubMed: 9127946]
48. Karp DA, Gittis AG, Stahley MA, Fitch CA, Stites WE, Lattman EE, Garcia-Moreno B. Molecular determinants of the abnormal pKa value of an internal aspartic acid: contributions by local unfolding and water penetration.
49. Nguyen DM, Leila RR, Gittis AG, Lattman EE. X-ray and thermodynamic studies of staphylococcal nuclease variants I92E and I92K: insights into polarity of the protein interior. J Mol Biol. 2004; 341:565–574. [PubMed: 15276844]
50. Stites WE, Gittis AG, Lattman EE, Shortle D. In a staphylococcal nuclease mutant the side-chain of a lysine replacing valine 66 is fully buried in the hydrophobic core. J Mol Biol. 1991; 221:7–14. [PubMed: 1920420]
51. Shortle D, Meeker AK. Mutant forms of staphylococcal nuclease with altered patterns of guanidine hydrochloride and urea denaturation. Proteins. 1986; 1:81–89. [PubMed: 3449854]
52. Neuman RCKWZA. Pressure dependence of weak acid ionization in aqueous buffers. J Phy Chem. 2004; 77:2687–2691.
53. Royer CA, Hinck AP, Loh SN, Prehoda KE, Peng X, Jonas J, Markley JL. Effects of amino acid substitutions on the pressure denaturation of staphylococcal nuclease as monitored by fluorescence and nuclear magnetic resonance spectroscopy. Biochemistry. 1993; 32:5222–5232. [PubMed: 8494899]

Author Manuscript Author Manuscript Author Manuscript Author Manuscript

54. Vidugiris GJ, Truckses DM, Markley JL, Royer CA. High-pressure denaturation of staphylococcal nuclease proline-to-glycine substitution mutants. Biochemistry. 1996; 35:3857–3864. [PubMed: 8620010]

55. Denisov VP, Schlessman JL, Garcia-Moreno EB, Halle B. Stabilization of internal charges in a protein: water penetration or conformational change? Biophys J. 2004; 87:398–3994.

56. Damjanovic A, Garcia-Moreno B, Lattman EE, Garcia AE. Molecular dynamics study of water penetration in staphylococcal nuclease. Proteins. 2005; 60:433–449. [PubMed: 15971206]

57. Frye KJ, Royer CA. The kinetic basis for the stabilization of staphylococcal nuclease by xylose. Protein Sci. 1997; 6:789–793. [PubMed: 9098888]

58. Walkenhorst WF, Green SM, Roder H. Kinetic evidence for folding and unfolding intermediates in staphylococcal nuclease. Biochemistry. 1997; 36:5795–5805. [PubMed: 9153420]

59. Hillson N, Onuchic JN, Garcia AE. Pressure-induced protein-folding/unfolding kinetics. Proc Natl Acad Sci U S A. 1999; 96:14848–14853. [PubMed: 10611301]

60. Bryngelson JD, Onuchic JN, Socci ND, Wolynes PG. Funnels, pathways, and the energy landscape of protein folding: a synthesis. Proteins. 1995; 21:167–195. [PubMed: 7784423]

61. Garcia AE, Onuchic JN. Folding a protein in a computer: an atomic description of the folding/unfolding of protein A. Proc Natl Acad Sci U S A. 2003; 100:13898–13903. [PubMed: 14623983]

62. Hummer G, Garde S, Garcia AE, Paulaitis ME, Pratt LR. The pressure dependence of hydrophobic interactions is consistent with the observed pressure denaturation of proteins. Proc Natl Acad Sci U S A. 1998; 95:1552–1555. [PubMed: 9465053]

Author Manuscript Author Manuscript Author Manuscript Author Manuscript

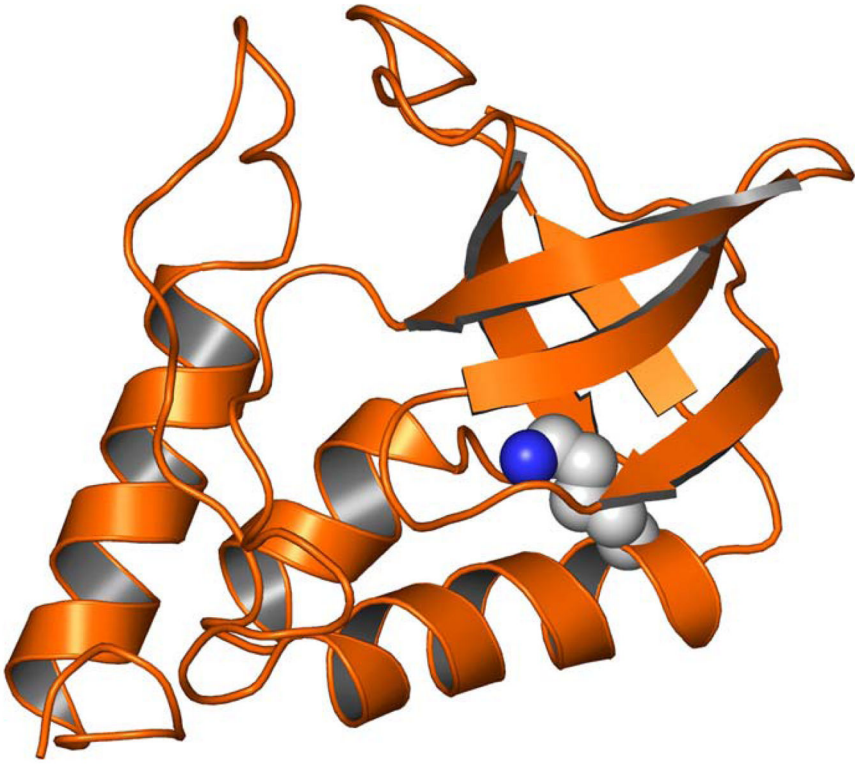

Figure 1.
Schematic of the structure of the SNase variant V66K with the residue K66 in space-filled representation (50).

Author Manuscript Author Manuscript Author Manuscript Author Manuscript

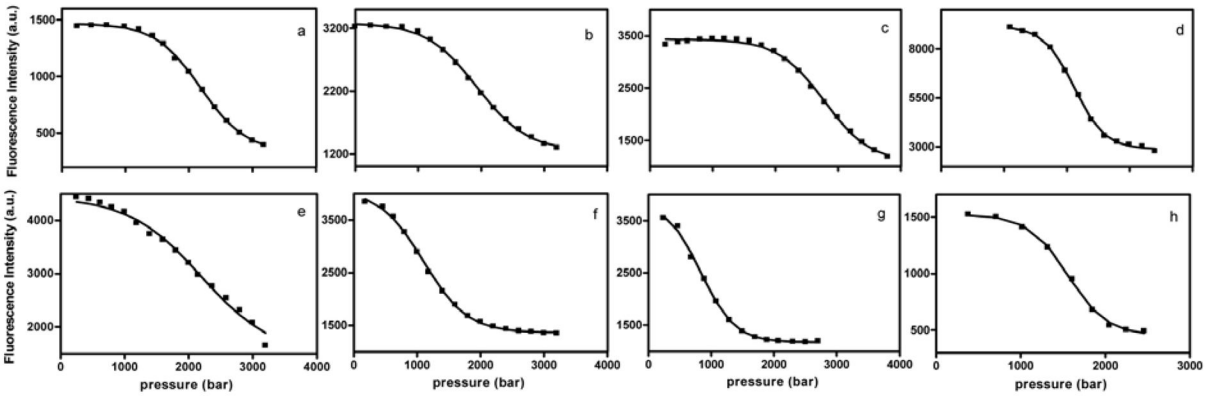

Figure 2.

Equilibrium fluorescence detected high pressure unfolding profiles for Snase and its variants. a.) WT Snase, b.) Δ+PHS+V66K, c.) Δ+PHS+V66D, d.) Δ+PHS+V66H, e.) Δ+PHS, f.) Δ+PHS+V66R, g.) Δ+PHS+V66E, h.) Δ+PHS+V66N. Conditions are given in Table 1. The temperature was 23 degrees C. Lines through the points represent fits to the data to equation 1 as described in the text.

Author Manuscript Author Manuscript Author Manuscript Author Manuscript

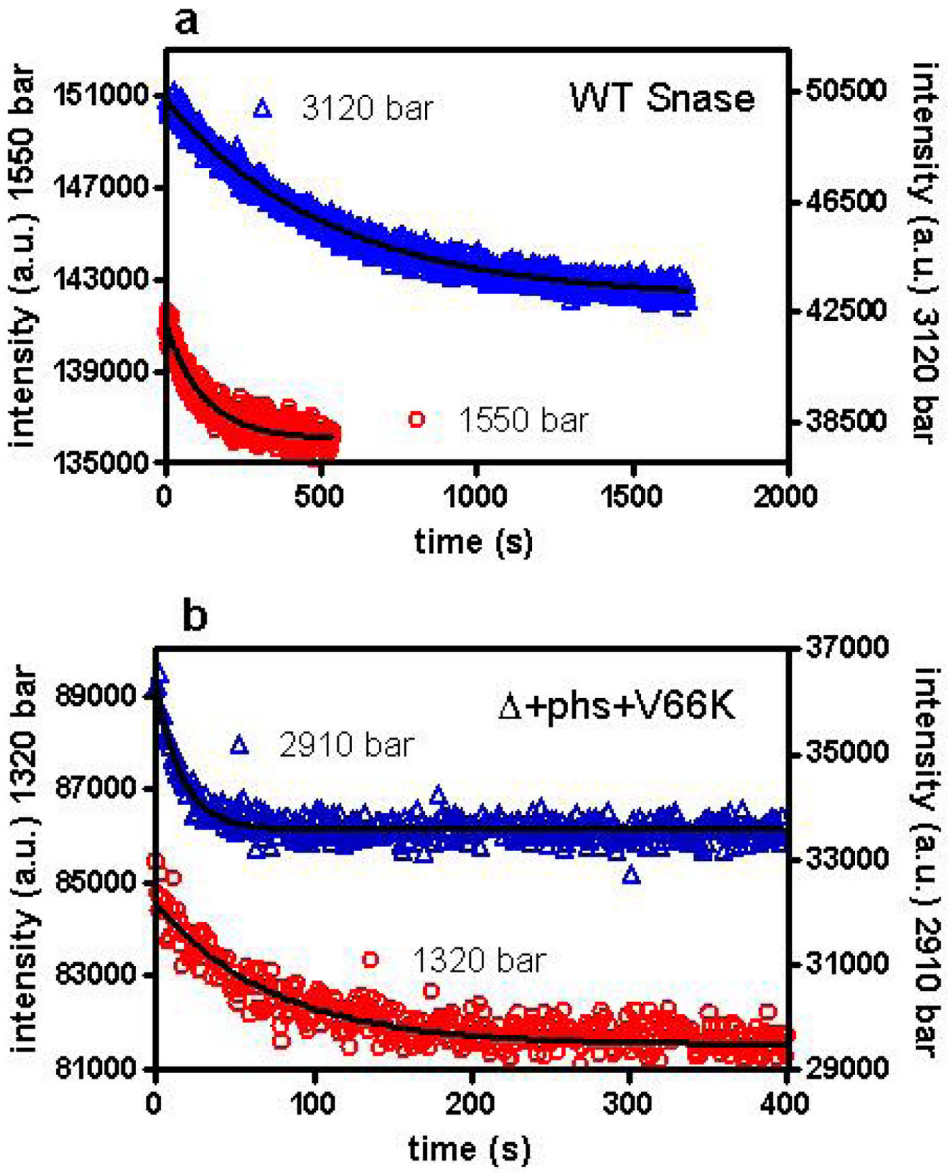

Figure 3.

Pressure jump fluorescence detected relaxation profiles a) WT Snase; (O) correspond to intensity relaxation after a jump from 1350 to 1550 bar, wheras (Δ) correspond to the relaxation after a jump from 2920 to 3120 bar. b) Δ+PHS+V66K variant, (O) correspond to intensity relaxation after a jump from 1100 to 1320 bar, wheras (Δ) correspond to the relaxation after a jump from 2710 to 2920 bar. The data were fit to a single exponential decay model (equation 4), and the lines drawn through the points correspond to the fits. Conditions are those in Figure 2. The data illustrate that for the wild type, relaxation slows significantly as pressure is increased, whereas for the Δ+phs+V66K variant, increasing pressure leads to much faster relaxation.

Author Manuscript Author Manuscript Author Manuscript Author Manuscript

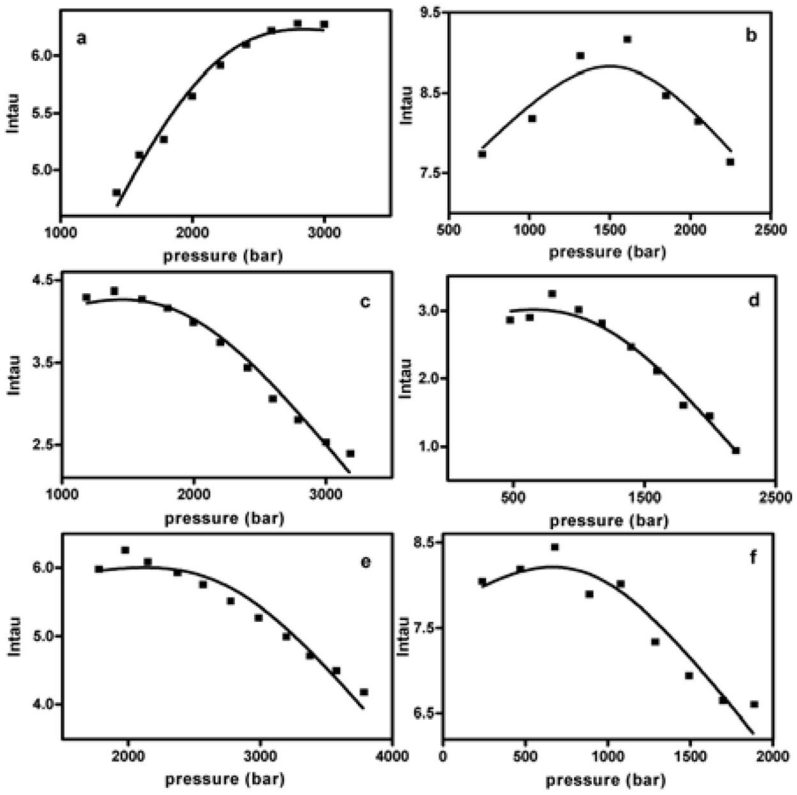

Figure 4.

Dependence of the natural logarithm of the relaxation time on the final pressure. The values for the relaxation times are those obtained from the fits of the data such as those in Figure 3. The lines through the points represent fits of the data according to equation 5, as described in the text. a.) WT Snase, b.) Δ+PHS+V66N, c.) Δ+PHS+V66K, d.) Δ+PHS+V66R, e.) Δ +PHS+V66D, f.) Δ+PHS+V66E.

Author Manuscript Author Manuscript Author Manuscript Author Manuscript

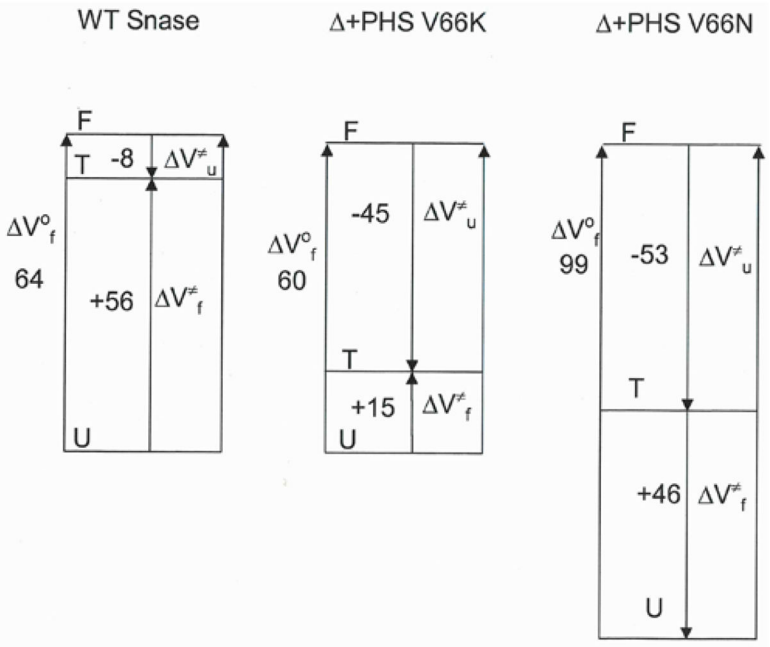

Figure 5.

Volume diagrams for the folding/unfolding reactions of WT Snase, and two of the variants Δ+PHS+V66K and Δ+PHS+V66N. The values for the activation volumes were obtained from the fits of the data such as those in Figure 4 and the equilibrium unfolding volume. All values were normalized to the same volume for the folded state, based on the fact that the structures of these proteins are nearly identical.

Author Manuscript Author Manuscript Author Manuscript Author Manuscript

Table 1

Volume changes for the folding/unfolding transitions of Snase cavity mutants

Protein	**WT Snase**	**Δ+PHS WT**	**Δ+PHS V66K**	**Δ+PHS V66R**	**Δ+PHS V66D**	**Δ+PHS V66E**	**Δ+PHS V66H**	**Δ+PHS V66N**
Conditions[a]	pH 6	pH 5 2M GuHCl	pH 6	pH 6	pH 8	pH 8 1 M GuHCl	pH 8 1 M GuHCl	pH 5 1 M GuHCl
ΔV^{o}_{f} (ml/mol)	64 ± 5	41 ± 4	60 ± 6	67 ± 5	62 ± 7	84 ± 10	94.0 ± 8	99 ± 14
$\Delta V^{\neq}_{f}$ (ml/mol)	56 ± 3	n.d.	15	14.6	9.5	30	52	46
$\Delta V^{\neq}_{u}$ (ml/mol)	−8	n.d.	−45 ± 3	−52 ± 4	−53 ± 4	−54 ± 8	−42 ± 8	−53 ± 9
ΔG^{o}_{f} (kcal/mol)	−3.6 ± 0.3	−2.3 ± 2	−3.0 ± 0.3	−1.9 ± 0.2	−4.4 ± 0.4	−1.8 ± 0.3	−5.1 ± 0.4	−4.0 ± 0.6
k^{o}_{f} (s^{-1})	0.28 ± 0.09	n.d.	0.03	0.06	0.01	4×10^{-4}	0.01	0.002
k^{o}_{u} (s^{-1})	6×10^{-4}	n.d.	1.9 (± 0.6) $\times 10^{-4}$	2.3 (± 0.5) $\times 10^{-3}$	2.6 (±1.3) $\times 10^{-6}$	1.9 (± 0.8) $\times 10^{-5}$	1.7 (± 1.5) $\times 10^{-6}$	1.9 (± 1.3) $\times 10^{-6}$

[a] – at pH below 7, the buffer used was 50 mM bis-Tris and above 7, the buffer was 50 mM Tris.